Performance Test of Various Discharge Chamber Configurations for ECR Discharge Ion Thruster*†

Haruya TOKI, Hajime FUJITA
Graduate School of Science and Technology Nihon University
1-8-14 Kanda Surugadai, Chiyoda, Tokyo, 101-8308, JAPAN
Telephone No. +81-42-759-8288
E-mail: htoki@ep.isas.ac.jp

Kazutaka NISHIYAMA, Hitoshi KUNINAKA, Kyoichiro TOKI
Institute of Space and Astronautical Science
3-1-1 Yoshinodai, Sagamihara, Kanagawa, 229-8510, JAPAN

Ikkoh FUNAKI
Institute of Engineering and Systems Tsukuba University
1-1-1 Tennodai, Tsukuba, Ibaraki, 305-8573, JAPAN

IEPC-01-107

The Institute of Space and Astronautical Science (ISAS) is developing a 20-cm-diam. Electron Cyclotron Resonance (ECR) discharge ion engine system, which is operated at a total power level of 1 kW and a thrust level of 30mN. This paper presents experimental results on the development of a 20-cm-diam ECR discharge chamber. This plasma generator utilizes samarium-cobalt magnets and microwave power at a frequency of 4.25GHz. The microwave power is introduced from a microwave power source via a coaxial cable followed by a coaxial-to-waveguide transformer. The performance of the device at its most optimum configuration features 500mA of extracted ion current, and 260eV/ion of discharge loss at a net microwave power of 130W.

Introduction

Electron bombardment ion thrusters comprise the most widely used type of ion engine. Its lifetime-critical parts are the main cathode and acceleration grid system and its performance is degraded due to erosion and electrode sputtering. Such ion thrusters require at least seven power supplies for the following functions: acceleration, deceleration, discharge, main-cathode heater, main-cathode keeper, neutralizer heater, and neutralizer keeper. Moreover, electron bombardment ion thruster systems are quite complex in terms of the required overall hardware structure, operating system, and operating procedure. On the other hand, microwave discharge ion thrusters produce plasma without the need of electrodes, thus being completely free from electrode erosion and contamination. Also, adoption of a microwave discharge as the ionization method greatly simplifies the overall system, as a single microwave amplifier can simultaneously generate a plasma in the both main plasma source and the neutralizer, having this two devices simply at a different potential from each other.

Microwave ion thrusters require four power supplies for the following functions: microwave generation, acceleration, deceleration and neutralizer heater energy supply, which in turn means that three to four power supplies are done away with, in comparison with the electron bombardment ion thruster system. This greater system simplicity brings about an increase in ion thruster lifetime, and results in a more simple and reliable overall thruster system. During the last few years, the ISAS electric propulsion division has developed a 10-cm-diam ECR discharge ion thruster (officially named mu-10 ion thruster), which has been operating successfully at a total power level

*Copyright © 2001 by Haruya Toki. Published by the Electric Rocket Propulsion Society with permission.
† Presented as Paper IEPC-01-107 at the 27th International Electric Propulsion Conference, Pasadena,CA,15-19 October,2001.

of 300 W, offering 7 mN of thrust. This 10-cm device comprises the primary propulsion system to be used for the MUSES-C asteroid sample return planetary probe, scheduled to be launched with the ISAS M-5 solid-propellant launcher in 2002. Following this technology demonstration mission, a high-performance ion engine operating at a higher thrust level will be required for future deep space science missions and, for this purpose, ISAS has started to develop a 20-cm-diam. ECR discharge ion engine operated at a power level of 1 kW and a thrust level of 30 mN. Such is the subject of the present study.

ECR discharge ion engines operate with lower thrust density than other thrusters, because the plasma density is limited by the so-called cut-off density. Accordingly, the overall diameter of the ECR ion engine must be increased if we wish to obtain higher thrust. A cross-sectional schematic of the mu-10 ion engine is shown in Figure 1(a). Now, in order to design a larger microwave discharge ion thruster, the following three concepts have been put forth, all of which have in common the usage of the same circular waveguide as the one employed by the mu-10 thruster.

The first concept involves increasing the axial length (or width) of the discharge chamber (Bucket type), as illustrated in Figure 1(b). Goede [1] adopted this method in developing a 30-cm-diam. ion source, featuring ECR heating at the neighborhood of the magnet surfaces. At high power operational levels, the plasma generation region was observed to shift to the central region of the discharge chamber, possibly due to electron anomalous diffusion. The highest ion production cost achieved by this device was 135eV/ion and, although the experimental tests assessing the thrust capabilities of this device have not been reported in his paper, it represents a configuration providing reasonable performance results. In subsequent work, Miyoshi [2] adopted a similar approach to develop the so-called Yoshino-II 10-cm-diam ion engine. However, due its low performance (400eV/ion of ion production cost and less than 80% of propellant utilization efficiency), this bucket-type concept was ultimately abandoned. Instead, after extensive experimental tests on 10-cm-diam class devices, the best performance was realized by reducing the distance between the ECR region and the screen grid, resulting in the adoption of a conical discharge chamber as depicted in Figure 1(a). Since the bucket-type approach has not been carried out for 20cm-class thrusters experiment, it remains to be seen whether this geometry will be effective for a larger diameter device as well.

The second possible concept comprises a discharge chamber inside of which a plasma ring is generated as shown in Figure 1(c). In this case, plasma generation occurs in a single place and complicated mode changes are not expected to occur readily. Still, in this device a large separating distance between the magnets is necessary and so, unless a magnet material which is more powerful than SmCo magnets is developed, it is unlikely that this concept will be materialized employing electric discharge chambers larger than 20cm in diameter. Also, although a plasma discharge can be started quite easily in such system, if a circular waveguide similar to the one used for the μ10 ion engine is utilized, matching adjustment of the microwave will become an issue which must be tackled properly so that microwave power will be transmitted efficiently. In any case, development of this concept is presently under way and the reader is referred to Ref. [3] for further details.

The third concept, being the one adopted in the present research, consists of a scaled up version (20-cm diam.) of the mu-10 device, maintaining the same magnet spacing but increasing the number of magnet rings and using a flat endplate as seen in Figure 1(d). Although performance levels equivalent to the ones obtained with the μ10 thruster are expected, since plasma generation takes place at several regions instead of a single one, instabilities produced by having a number of possible microwave resonance modes may become an issue. Furthermore, taking into account the short discharge chamber width, the larger the number of magnets on the flat endplate, the larger will be the degradation of the Q-value of such chamber.

In this study, the efficiency of several ion engine configurations, featuring different discharge chamber geometries and a variety of magnetic circuit layouts, as well as propellant supply port set-ups, have been compared and the overall performance of 20-cm-diam. ECR discharge ion thruster has been evaluated. In the near future, scaling-up of the 10-cm ECR ion thruster is being envisaged at ISAS for latter use in actual missions. This work represents a first step in that direction.

Experimental set-up

Figure 2 shows a cross-sectional view of the 20-cm-diam ion thruster. Its magnetic circuit is a so-called

flat-type circuit, generating a number of ring-cusped magnetic fields at which plasma is generated. The discharge chamber is composed of a flat-disk shaped end-plate made out of steel. Grooves have been cut out on the surface of this end-plate in order to accommodate the Samarium Cobalt permanent magnets. It also features an aluminum circular waveguide. The chamber depth, waveguide length, and layout of the magnetic circuit can be varied just by replacing the pertinent parts. The experimental set up is depicted in Figure 3. The ECR discharge is produced by a 4.25GHz microwave signal, and magnetic fields of strength up to 4.5kG are present inside the discharge chamber. This microwave signal, being generated by a TWT amplifier, is injected through a circular waveguide attached to the endplate of the discharge chamber.

A plunger located upstream of the waveguide can be easily adjusted in order to keep the reflected power to a minimum. The ion source can be electrically insulated with a DC cutter, which is located right before the connecting point of the microwave coaxial cable with the device. In this device, insulation is achieved by having the DC cutter positively with respect to the power supply. However, since experiments involving beam extraction by a grid system have not been carried out, this DC cutter has not been used. The vacuum chamber is 1.5m in diameter and 2.5m in length, and is evacuated via two oil diffusion pumps yielding 12,000liter/sec vacuum capacity. The propellant gas is Xenon and the total gas flow rate for all experimental tests in this work is set to 6sccm. For such propellant flow rate setting, the lowest achieved vacuum level was 1.6×10^{-5} Torr.

Experimental Results and Discussion

Magnetic Circuit Layout

In the first part of this research, several different magnet configurations have been investigated. The ion source has an axial width of approximately 30 mm and the width in the axial direction of the magnets aligned inside the endplate grooves (herein referred as magnet rows) is 12 mm. Ion beam optics ensure that the ECR regions are generated right next to the magnets. The ion extraction current has been measured using a punching metal plate, as shown in Figure 2. Since none of the tested configurations achieved self-ignition, a tungsten filament biased at a -100V was placed outside of the discharge chamber. This filament was heated by a current of 8A, thus generating electron thermal emission. A snapshot of the microwave discharge can be viewed in Figure 4.

Figure 5 shows four representative magnetic circuits tested so far, and the results stemming from the performance evaluation experiments are given in Figures 6 through 8. After an extensive trial and error assessment, it was concluded that configuration type D offered the highest ion current values of all four cases. The discharge chamber axial width, being one of the experimental parameters, was found to be most optimum at a value of 30mm. Axial widths longer or shorter than this value either affected the performance or resulted in unstable operation. Figure 9 shows the magnetic field strength distribution, numerically calculated for configuration type D. For a 4.25GHz input microwave signal, the resonance magnetic field is estimated to be 0.15T. Such magnetic field strength is found to be at a location 13 mm from the collecting grid surface and 5 mm from the surface of the magnets. It needs to be pointed out that increasing the spacing between the two innermost annular magnet rows produces a decrease in magnetic field strength, which promotes relatively low microwave power absorption efficiency in this inner region of the discharge chamber and enables microwave power to reach the regions next to the outer magnet rows. The purpose of having a sort of bridge between the external rows in configuration type D is to enable plasma production to take place right in front of the outer magnet rows. This bridge enables electrons to reach the outer magnetic row regions as they describe a drifting motion [4, 5, 6], thus compensating the decrease in microwave electric field strength.

A doughnut-shaped plasma region and two crescent-shaped plasma regions are created in the inner radial and outer radial regions of the discharge chamber, respectively (Figure 4). In order to take advantage of the individual characteristics of both configuration type B (featuring inner magnetic rows only) and type C (featuring outer magnetic rows only), the geometries of these two types were amalgamated to conform the most optimum configuration (type D). The variation of the ion production cost with input microwave power is shown in Figure 7. The ion production cost C_i is defined as follows,

$$C_i = \frac{P_f}{I_b}$$

where P_f is the net microwave power being supplied to the ion source and I_b is the extracted ion current. The ion production cost increases in an almost linear fashion and is proportional to the input microwave power, showing a tendency which is typical of ion engine systems. Since the ion beam was not extracted in these experiments, the neutral pressure was kept constant for all cases with a xenon flow rate of 6 sccm, regardless of the ion currents to the punching metal. If the difference of microwave standing wave modes and E-field intensities in the discharge chamber in configuration types B, C and D is neglected, we might expect an ion current of 600 mA at a microwave power of 120W, which is the summation of the ion current in case B (230 mA @ 40 W) and the one in case C (370 mA @ 80 W). "The ideal performance" curve shown in Figure 6 was calculated by adding the baseline ion current of 230 mA produced in the configuration type B at 40 W to the ion currents generated in the configuration type C at microwave powers of 35~80 W.

Since configuration types B and C both contain regions where purposely no plasma generation takes place, the existing electric field strength becomes high, resulting in relatively high plasma production efficiencies. However, in configuration type D, plasma production occurs in the whole discharge chamber, and so the relatively weak electric field is responsible for the lower plasma production efficiencies obtained in this case. Configuration type A is similar to type B, except for the fact that the innermost magnet row has been shifted inwards to a ring of smaller diameter.

Even though the operational range for the input microwave power in configuration type A decreased, experiments show that it provides ion current and ion production cost values similar to the ones obtained for configuration type B. Figure 8 shows the dependence of ion current density on plasma generation area for a number of input power settings. It is seen that configuration type D yields the lowest current density levels of all four configuration types, possibly due to the lower existing electric field strength. Comparing results for configuration types A and B, it is observed that although both types yield almost the same ion current and ion production cost values, the former configuration of the two provides higher current density levels. As seen in Figure 8, the current density values differ depending on the configuration type being employed. Considering that the input microwave frequency was the same for all configurations, it may be concluded that the cut-off density was not reached in any of experimental tests. Whereas the current densities obtained with the μ10 ion thruster fall within the 1.8~2.8 mA/cm^2 range, configuration type A provides at least twice as high a current density level, falling in the 4.0~4.3 mA/cm^2 range. It should be pointed out that having a 10-cm ion thruster with a current density level similar to the one obtained with the configuration type A would be a promising thruster system deserving serious consideration.

Comparing plasma generation efficiencies, at first glance it would be desirable to have the inner magnetic rows of configuration type D conforming a pattern same as the one adopted in configuration type A. However, such pattern has not been chosen because it would involve greater amounts of microwave power absorption taking place in the inner region of the discharge chamber, thus preventing the microwave power from reaching the radially-outward zones where the outer magnet rows are located.

Gas Port Configuration

Since the axial width of the discharge chamber of our 20cm thruster is relatively short (30 mm), a non-uniform neutral gas pressure distribution is expected to exist inside the discharge chamber when the propellant is fed in. Furthermore, since feeding the propellant only in the axial direction through the waveguide would result in having a relatively large amount of propellant being ejected downstream without being ionized, in addition to the two main inner ports, four gas ports were installed on the side wall of the discharge chamber, facilitating the spreading of the propellant more evenly throughout the discharge chamber. Although in Figure 10 these outer ports are shown at the top and bottom, all four ports are located at 90 degrees from each other and facing towards the central axis of the device.

The amount of propellant gas flowing into the discharge chamber from the different ports was controlled independently. By doing so, the ratio of propellant flowing through the gas ports located inside (also referred herein as inner ports) to the amount of propellant being fed from the gas ports located in the side wall (also referred herein as outer ports) was varied and its effect on performance was investigated. Such ratio is herein referred as gas supply ratio.

Figure 11 shows the variation of the ion current with gas supply ratio. For any given input microwave

power level, a supply ratio of 3:3 (3 sccm through inner ports and 3 sccm through outer ports) offers the highest ion current values. In Figure 12 the variation of discharge loss with gas distribution is presented, and it may be observed that a gas supply ratio of 3:3 produces the lowest amount of discharge loss. Therefore, it is concluded that a 3:3 gas supply ratio is the most optimum one. The amount of ion current collected was also compared in the following two cases: a) gas supply through the inner ports only; b) 3:3 gas supply ratio and results are shown in Figure 13. Obviously, the ion current is higher when setting the propellant gas distribution to a 3:3 ratio for all microwave power levels tested in this experiment. The improvement in plasma production efficiency for a 3:3 gas supply ratio may be explained by inferring that since half the amount of neutral gas is introduced from inside and the other half is fed from the outside, the tendency for the neutral gas to concentrate inside the discharge chamber due to the pressure difference decreases. Thus, configuration type D with a 3:3 gas supply ratio setting yielded the best performance results (530mA of total extracted ion current for an microwave input power of 130W).

Conclusion

The experimental results for a 20-cm-diam. microwave discharge ion thruster using Xe as the propellant gas have been presented. A discharge chamber with an axial width of 30 mm was found to the most optimum one. Several magnet row configurations were investigated and the best performance was attained with a geometry consisting of several magnet rows producing three segmented plasma rings. In this most optimum configuration (type D), the following plasma generation zones were established: 1) a doughnut-shaped plasma region located around the waveguide exit, where the slightly larger separating distance between the magnet rows assured moderate microwave absorption levels in this zone, and 2) two crescent-shaped plasma rings surrounding the previous one, where a comparatively smaller distance between the magnet rows effectively produced a plasma with relatively weak electric field intensity at the outer region of the discharge chamber. The ion current collected by the negatively-biased metallic grid was 480 mA for a net input microwave power of 100 W. Four propellant-feed ports were installed in the side-wall, resulting in a total of six ports being utilized. By setting the propellant flow rates to be the same for both inner-port and outer-port feeding, an improvement in thruster performance was attained resulting in generated ion currents of up to 500 mA at a net input microwave power of 130 W.
Considering that our final goal is to obtain an ion current of 600 mA at an input microwave power setting of 120W with a 20-cm diameter chamber, it is believed that such performance level may be difficult to achieve by launching the microwave signal into the discharge chamber via only one central waveguide. Therefore, further development efforts will concentrate on new microwave insertion methods.

References

[1] H. Goede, "30-cm Elect Cyclotron Plasma Generator," *Journal of Spacecraft and Rockets 24*, 5, 437-443, September-October 1987.

[2] H. Miyoshi, S. Ichimura, H. Kuninaka, K. Kuriki. and Y.Horiuchi, "Microwave Ion Thruster with Electron Cyclotron Resonance Discharge" *22nd International Electric Propulsion Conference, IEPC-91-084, Viareggio, Italy* ,October 14-17, 1991

[3] I. Funaki, K. Nishiyama, H. Kuninaka, K. Toki, Y. Shimizu, and H. Toki, "20mN-class Microwave Discharge Ion Thruster" *27th International Electric Propulsion Conference, IEPC-01-103, Pasadena, USA* ,October 15-19, 2001

[4] H.Kuninaka, N.Hiroe, K.Kitaoka, Y.Ishikawa, K.Nishiyama and Y.Horiuchi, "Development of an Ion Thruster System for Interplanetary Missions" *23rd International Electric Propulsion Conference, IEPC-93-198, Seattle, USA* ,September 13-16, 1993

[5] H.Kuninaka and Y.Horiuchi, "System Operation of Microwave Discharge Ion Thruster" *30th AIAA/ASME/SAE/ASEE Joint Propulsion Conference, AIAA-94-3239, Indianapolis, USA*, June 27-29, 1994

[6] K. Nishiyama, S. Satori, H.Kuninaka and K. Kuriki, "Plasma Diagnostics inside a Microwave Discharge Ion Thruster Using Tunable Laser Diodes" *24th International Electric Propulsion Conference, IEPC-95-190, Moscow, Russia,* September 19-23, 1995

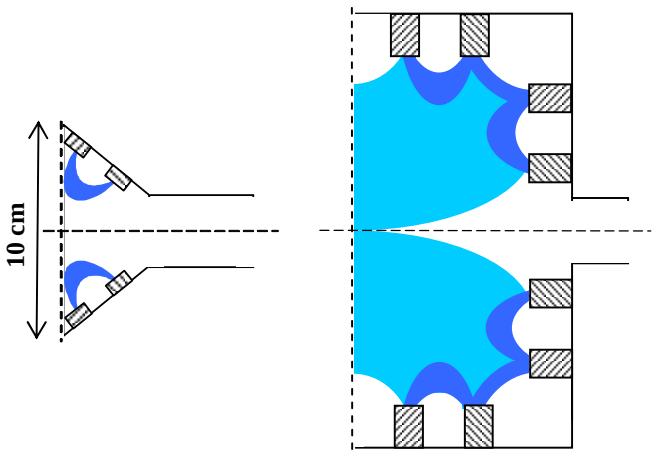

(a) μ10 (b)Bucket type

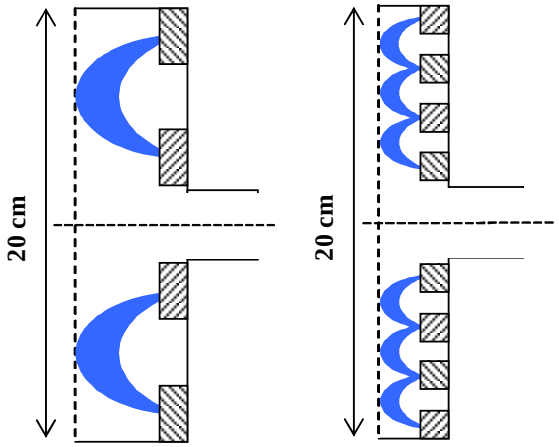

(c)Single type (d)Multi type

Figure 1. Discharge layout concepts

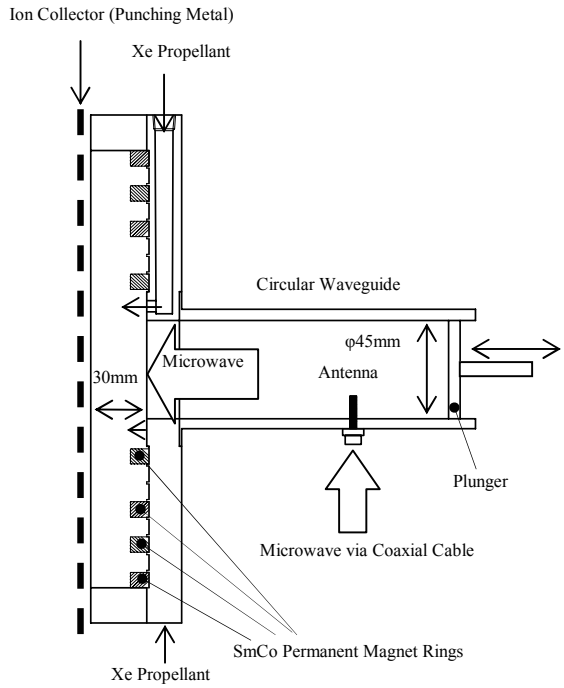

Figure 2. Cross Sectional View of 20cm-Class Ion Thruster

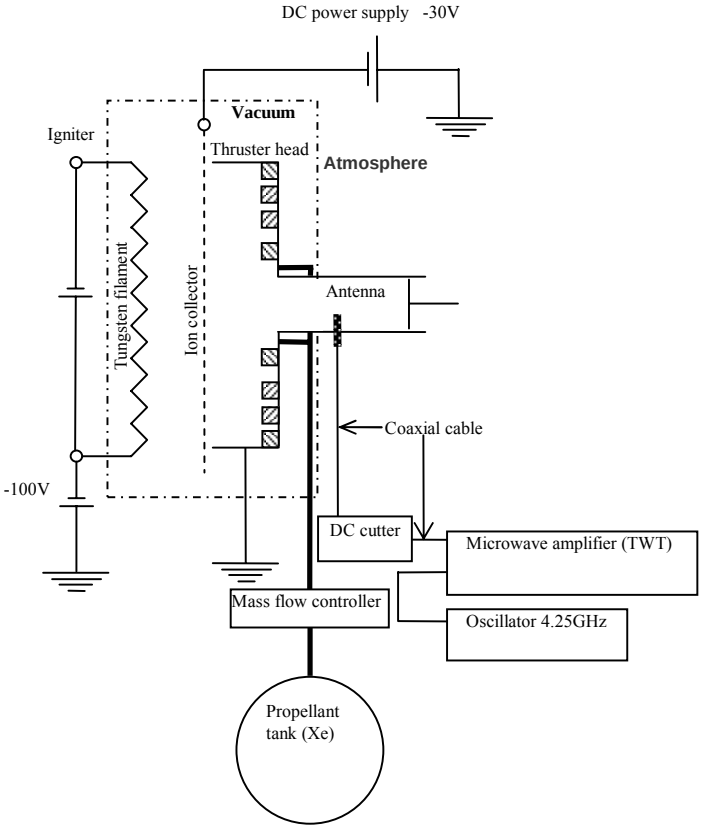

Figure 3. Experimental Setup

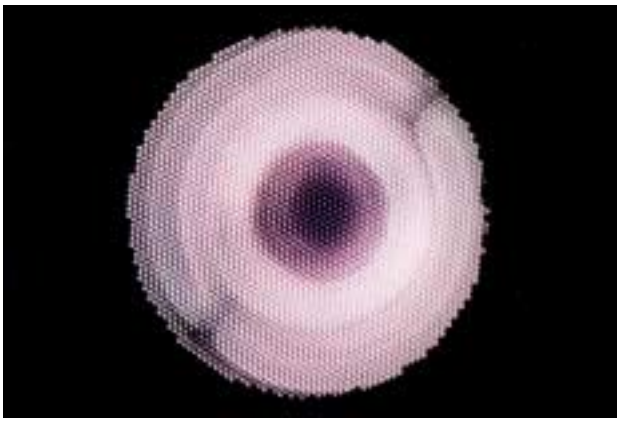

Figure 4. Snapshot of Plasma Discharge

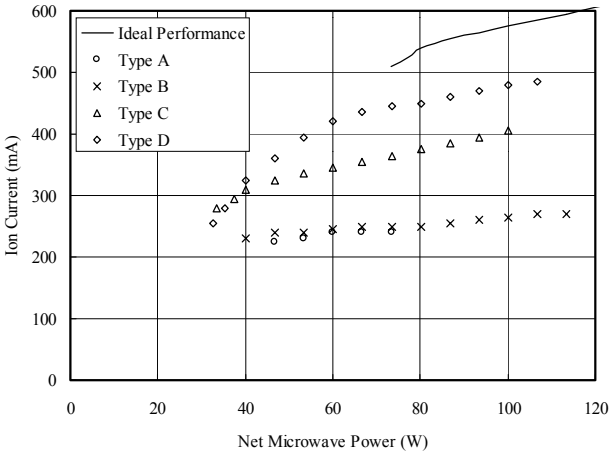

Figure 6. Ion Current Variation with Microwave Power

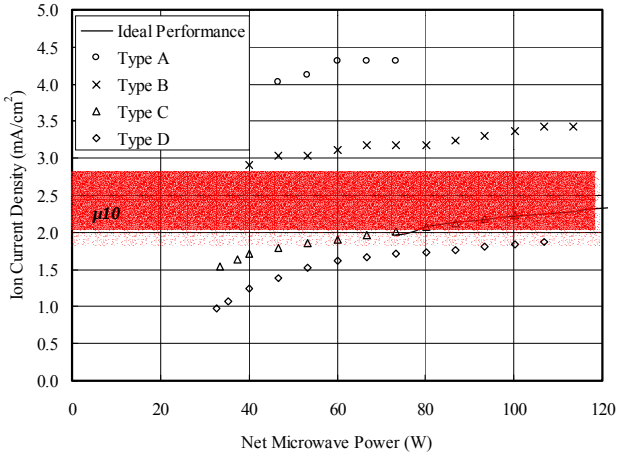

Figure 8. Ion Current Density Variation with Microwave Power

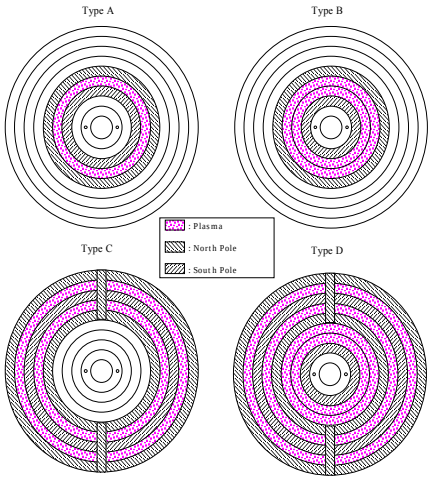

Figure 5. Magnet Circuit Configuration Types

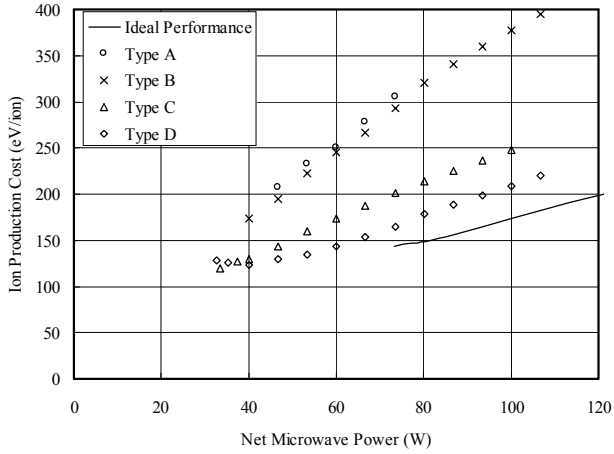

Figure 7. Ion Production Cost Variation with Microwave Power

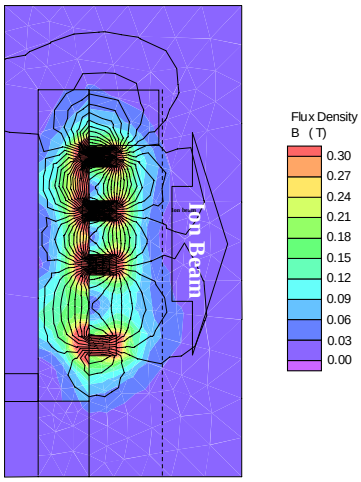

Figure 9. Magnetic Field Profile (Config. Type D)

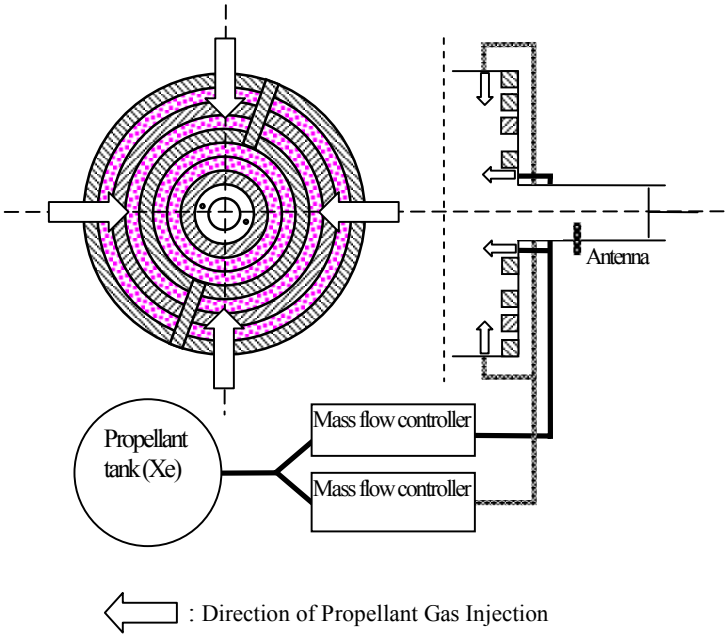

Figure 10. Gas Port Configuration

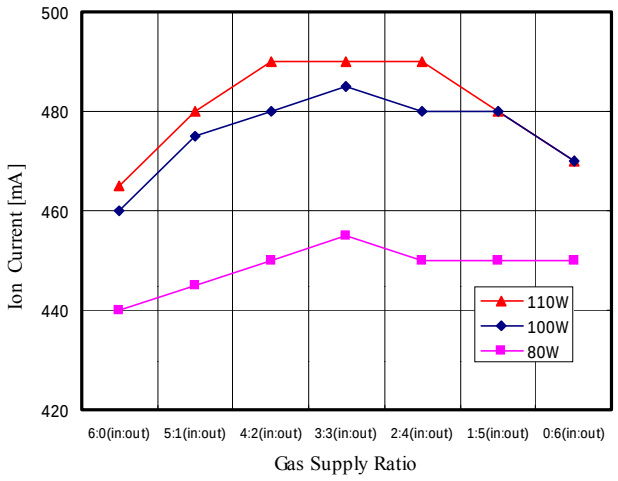

Figure 11. Ion Current Variation with Gas Supply Ratio

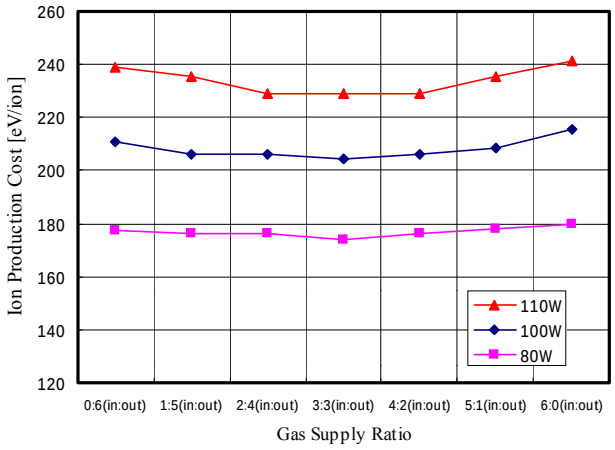

Figure 12. Ion Production Cost Variation with Gas Supply Ratio

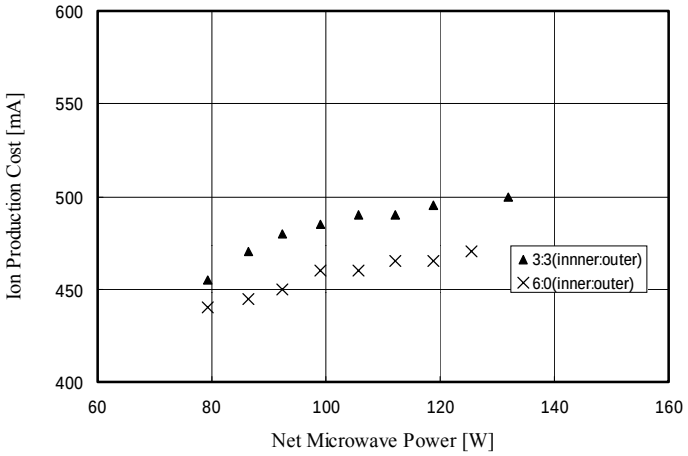

Figure 13. Comparison between 3:3 and 6:0 Gas Supply Ratio Results